

FIG. 7. Dependences of $\ln r^*(T)$ on T^{-1} for: a) Al+0.048 at.% Ag; b) Cu+0.17 at.% Al. In Fig. 7a we have $r^*(T) = [\rho_d(T) - \rho_{d\min}]/\rho_{d\min}$. The numbers alongside the curves give the numbers of the samples of the alloys (compare with Figs. 4 and 1).

slightly distorted and do not have an abrupt step, Eq. (2) describes the rise of $r(T)$ from the minimum to almost the point of transition to a plateau (case a in Fig. 7).

The energy ϵ calculated from Eq. (2) is within the range $(0.7-1.2) \times 10^{-2}$ eV for the various Cu alloys and it amounts to $(1.3-1.7) \times 10^{-2}$ eV for the Al alloys. In the case of samples with different dislocation structures the value of ϵ varies somewhat and clearly the alloys are characterized by higher values of ϵ than the weakly deformed pure metals.^[2-3]

Our experiments give information mainly on the scattering by high-frequency vibrations. Clearly, the experimental results give some particular value of ϵ governed by the position of the maximum of the spectral density of phonons in the short-wavelength region. In this case the value of ϵ is determined by the characteristic frequency ω of the quasilocal vibration modes of dislocations. The temperature position of the step suggests that the characteristic frequency of these vibrations should be between 2 and 3 times less than the

Debye frequency.

The results of our measurements show that if L_f is less than 30 lattice periods, achieved in our experiments by the addition of Mg to aluminum or of Pt and Rh to copper, the characteristic dislocation scattering channel is then suppressed.

¹Estimates are made on the basis of the value of $\rho_d(4.2^\circ\text{K})$. In the case of copper we find that $\rho_d(4.2^\circ\text{K})/N \approx 1.8 \times 10^{-19} \Omega \cdot \text{cm}^3$ (Ref. 5) and in the case of aluminum it is $\rho_d(4.2^\circ\text{K})/N \approx 1.8 \times 10^{-19} \Omega \cdot \text{cm}^3$ (Ref. 6) (N is the dislocation density). The presence of impurities should not alter significantly the value of this ratio.^[7]

- ¹J. Bass, *Adv. Phys.* **21**, 431 (1972).
²V. F. Gantmakher and G. I. Kulesko, *Zh. Eksp. Teor. Fiz.* **67**, 2335 (1974) [*Sov. Phys. JETP* **40**, 1158 (1975)].
³G. I. Kulesko, *Zh. Eksp. Teor. Fiz.* **72**, 2167 (1977) [*Sov. Phys. JETP* **45**, 1138 (1977)].
⁴R. S. Seth and S. B. Woods, *Phys. Rev. B* **2**, 2961 (1970).
⁵V. F. Gantmakher, V. A. Gasparov, G. I. Kulesko, and V. N. Matveev, *Zh. Eksp. Teor. Fiz.* **63**, 1752 (1972) [*Sov. Phys. JETP* **36**, 925 (1973)].
⁶J. G. Rider and C. T. B. Foxon, *Philos. Mag.* **13**, 289 (1966).
⁷A. B. Bhatia and O. P. Gupta, *Phys. Rev. B* **1**, 4577 (1970).
⁸P. R. Suon, in: *Elektronnaya mikroskopiya i prochnost' kristallov*, pod red. prof. D. A. Petrova (*Electron Microscopy and Strength of Crystals*, ed. by Prof. D. A. Petrov), *Metallurgiya*, M., 1968, p. 123.
⁹J. Friedel, *Dislocations*, Pergamon Press, Oxford, 1964 (Russ. transl., Mir, M., 1967, p. 343).
¹⁰I. M. Lifshitz and A. M. Kosevich, Preprint No. 170/T-025, Physicotechnical Institute, Academy of Sciences of the Ukrainian SSR, Kharkov, 1965.
¹¹Ya. A. Iosilevskii, *Pis'ma Zh. Eksp. Teor. Fiz.* **7**, 32 (1968) [*JETP Lett.* **7**, 22 (1968)].
¹²G. G. Taluts, A. Ya. Fishman, and M. A. Ivanov, *Fiz. Tverd. Tela (Leningrad)* **13**, 3572 (1971) [*Sov. Phys. Solid State* **13**, 3016 (1972)].
¹³M. A. Ivanov, G. G. Taluts, and A. Ya. Fishman, *Fiz. Met. Metalloved.* **31**, 260 (1971).

Translated by A. Tybulewicz

Passage of current through a Josephson barrier of finite dimensions

S. A. Vasenko and G. F. Zharkov

P. N. Lebedev Institute of Physics, USSR Academy of Sciences

(Submitted 7 December 1977)

Zh. Eksp. Teor. Fiz. **75**, 180-190 (July 1978)

The static solutions of the nonlinear differential equation describing the current distribution in a Josephson barrier of finite width are studied. All the possible types of distributions are described, and the stability of the obtained solutions is investigated. It is shown that the solutions corresponding to the presence of excited vortex states in junction with a transport current are unstable and, therefore, cannot be realized under ordinary conditions. Examples are given of self-oscillating solutions, which arise in a junction with a current whose strength exceeds the critical value. The dependence of the period of the self-oscillations on the parameters of the problem has been determined with the aid of a computer.

PACS numbers: 74.50. + r

1. The problem of the nature of the passage of a current through a Josephson barrier of finite width in the absence of an external (current-unrelated) magnetic field was considered earlier by Owen and Scalapino,^[1]

who, by numerically integrating the corresponding nonlinear differential equation, found, in particular, that in a wide barrier the transport current is largely concentrated near the barrier edges and does not penetrate

to the middle, as a result of which there arises a current self-limiting effect.¹⁾ (The current self-limiting effect was first pointed out in Ferrel and Prange's paper⁽⁶⁾.)

The present paper is devoted to a more detailed consideration of the problem. The detailed analysis carried out by us allowed the discovery of the existence of other solutions, in addition to the ones described in Refs. 1 and 2. Thus, for example, below we show that for a sufficiently wide barrier in the absence of an external field there exist solutions describing anomalous (as compared with those presented in Refs. 1 and 2) current distributions, when the transport current flows mainly in the middle of the barrier, decreasing toward the barrier boundaries, as well as more complex distributions, when the currents in different sections of the barrier flow in opposite directions (see Fig. 1c below). Such excited current states are similar to vortices produced in a wide barrier upon the application to it of an external magnetic field.⁽³⁻⁵⁾ The analysis carried out by us (see below) shows, however, that such anomalous distributions are unstable, only normal states of the type described in Refs. 1 and 2 being stable. For this reason the anomalous distributions cannot, under ordinary conditions, be realized in experiment. Nevertheless, below we describe both the normal and anomalous distributions, since the latter form part of all the possible solutions of the static

(time-independent) problem. It is also possible that these unstable distributions will be of interest under some specific conditions.

In Sec. 2 we give an account of all the possible types of current and field distributions in a Josephson barrier of finite width (we consider the static case). In the present paper the boundary-value problem for the nonlinear equation governing the field and current distributions in the junction is reduced to the equivalent Cauchy problem (cf. Ref. 5), which allows us to uniquely associate with each solution a definite set of "initial" data (i.e., the value of the function and the value of its derivative at one of the boundaries of the barrier). Integral relations are found which allow the determination of the "initial" data in terms of the parameters of the boundary-value problem. The dependences, obtained with the aid of a computer (and, in a number of cases, analytically: see Sec. 3), are illustrated graphically.

In Sec. 4 we investigate the question of the stability of the obtained solutions. As has already been noted, the analysis carried out by us showed that only the ordinary Meissner-type solutions^(1,2) (corresponding to a monotonic decrease of the field from the boundaries to the center of the barrier) are stable. All the anomalous solutions turned out to be unstable. The result that the anomalous solutions are unstable is supported by the results of the investigation of the dynamics of the development of the solutions of the corresponding time-dependent nonlinear equation.

In Sec. 5, with the aid of a numerical solution of the nonstationary equation, we present examples of self-oscillating solutions arising in the barrier upon the passage of current of strength higher than the critical value and find the dependences of the period of the self-oscillations on the parameters of the problem.

2. The basic equation describing the steady-state field and current distributions in a Josephson barrier has the form⁽¹⁻⁷⁾

$$d^2\varphi/dx^2 = \sin\varphi. \quad (1)$$

The quantity $\varphi(x)$ (the so-called phase difference of the wave functions of the superconductors) is connected with the magnetic field in the barrier:

$$d\varphi/dx = H(x). \quad (2)$$

In (1) and (2) we have used dimensionless quantities: the coordinate is measured in units of λ_J ($\lambda_J \sim 0.1 - 1$ mm is the characteristic penetration depth of the field into the weak superconductor); the magnetic field is measured in units of $H_J = \Phi_0/2\pi\lambda_J\Lambda$ ($\Phi_0 = 2 \times 10^{-7}$ G-cm² is the magnitude of a flux quantum and $\Lambda \sim 10^{-5}$ cm is the penetration depth of the field into the bulk superconductor; normally $H_J \sim 0.1 - 1$ G); the density of the current passing through the barrier is equal to $j = j_c \sin\varphi(x)$, where j_c is the maximum value of the current density. We consider the one-dimensional problem, when the current flows along the x axis and depends only on the x coordinate in the plane of the barrier.

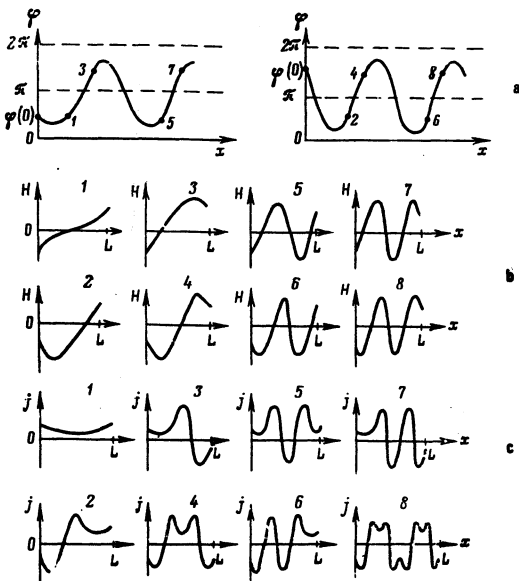


FIG. 1. a) Schematic representation of the "bounded" solutions (5) of Eq. (1). The value of the phase at $x=0$ is denoted by $\varphi(0)$ and $d\varphi/dx|_{x=0} = -H_1$. The two cases correspond to two possibilities: $0 < \varphi(0) < \pi$ and $\pi < \varphi(0) < 2\pi$. The points on the curves where the derivative assumes the value $d\varphi/dx|_{x=L} = H_1$ in accordance with (3) are indicated. The numbers by these points correspond to the solution numbering system used in the present paper. For example, solution No. 3 is represented by the section of the curve between the point $\varphi(0)$ and the point 3, and similarly for the other solutions. It is clear that in this way all the possible solutions of the problem can be enumerated. b) The $H(x) = d\varphi/dx$ field distributions for the various solutions; the numbers by the curves are the numbers of the solutions. c) Possible distributions of the current $j = \sin\varphi$ in the junction (schematic).

The boundary conditions for the problem of the passage of a total current I through a barrier of width L in the absence of an external magnetic field have the form

$$\left. \frac{d\varphi}{dx} \right|_{x=0} = -H_I, \quad \left. \frac{d\varphi}{dx} \right|_{x=L} = H_I, \quad (3)$$

where H_I is the self-magnetic field of the current, connected with the total transport current, I , by the relation

$$H_I = I/2 \quad (4)$$

(in dimensional units the relation (4) assumes the normal form $H_I = 4\pi I/c$; we assume that $I > 0$).

Equation (1) has a general solution in the form of an elliptic integral, giving in an implicit form the function $\varphi(x)$ (cf. Ref. 5):

$$x = \frac{1}{2} \int_{\varphi(0)}^{\varphi(x)} \frac{dy}{\xi(y)R(y)}, \quad H(x) = 2\xi(x)R(\varphi(x)),$$

$$R(y) = \left[\sin^2 \frac{y}{2} - \sin^2 \frac{B}{2} \right]^{1/2}, \quad \sin^2 \frac{B}{2} = \sin^2 \frac{\varphi(0)}{2} - \frac{H_I^2}{4} \quad (5)$$

$$\xi(x) = \text{sign } H(x) = \pm 1,$$

where the conditions (3) have been taken into account. The solutions $\varphi(x)$ can be expressed in terms of the Jacobi elliptic functions, but we prefer to deal directly with the integral representation (5). It is not difficult to verify that solutions of the type (5) correspond to a finite phase $0 \leq |\varphi(x)| \leq 2\pi$ (see Fig. 1a), the solution oscillating as the coordinate is varied,²⁾ while the field $H(x) = d\varphi/dx$ can change its sign along the junction (see Fig. 1b). Since the solution of the problem (1)–(3) is determined only modulo 2π (i.e., to the solution can always be added the constant $2\pi m$), we can, without loss of generality, consider the interval $0 \leq \varphi(x) \leq 2\pi$ the domain of variation of $\varphi(x)$ (see Fig. 1a).

According to (3), we have $H^2(0) = H^2(L) = H_I^2$; therefore, the function $\varphi(x)$ in (5) should satisfy the relation $\sin^2[\varphi(0)/2] = \sin^2[\varphi(L)/2]$, from which, with allowance for the requirement that $0 \leq \varphi(x) \leq 2\pi$, we have two possibilities: $\varphi(L) = \varphi(0)$ or $\varphi(L) = 2\pi - \varphi(0)$. In accordance with these possibilities, the solutions to Eq. (1) can satisfy two conditions that follow from (5):

$$L = \frac{1}{2} \int_{\varphi(0)}^{\varphi(L)} \frac{dy}{\xi(y)R(y)}, \quad \varphi(L) = \varphi(0) \quad (6)$$

or

$$L = \frac{1}{2} \int_{\varphi(0)}^{\varphi(L)} \frac{dy}{\xi(y)R(y)}, \quad \varphi(L) = 2\pi - \varphi(0). \quad (7)$$

Notice that if we define the quantity B in (5) as the principal value of the arc sine, i.e., if

$$B(\varphi_0) = 2 \arcsin \left\{ \sin^2(\varphi(0)/2) - H_I^2/4 \right\}^{1/2}, \quad (8)$$

then the values of $\varphi(x)$ at the points x_{\min} and x_{\max} corresponding to the extrema of $\varphi(x)$ are equal to

$$\varphi(x_{\min}) = B, \quad \varphi(x_{\max}) = 2\pi - B, \quad H(x_{\min}) = H(x_{\max}) = 0.$$

With allowance for this remark, the relations (6), (7) can be rewritten in the form

$$L = J_N(\varphi_0), \quad N=1, 2, 3, 4, \dots, \quad (9)$$

where we have set $\varphi_0 \equiv \varphi(0)$ and

$$J_{4n+1}(\chi) = U(\chi) + nW(\chi), \quad J_{4n+3}(\chi) = U(\chi) + 1/2 V(\chi) + nW(\chi), \quad 0 \leq \chi \leq \pi;$$

$$J_{4n+2}(\chi) = U(\chi) + 1/2 V(\chi) + nW(\chi), \quad J_{4n+4}(\chi) = U(\chi) + nW(\chi), \quad \pi \leq \chi \leq 2\pi;$$

$$U(\chi) = \int_{B(\chi)}^{\chi} \frac{dy}{R(y)}, \quad V(\chi) = \int_{\chi}^{2\pi-\chi} \frac{dy}{R(y)}, \quad W(\chi) = \int_{B(\chi)}^{2\pi-B(\chi)} \frac{dy}{R(y)}, \quad (10)$$

$$R(y) = \left[\sin^2 \frac{y}{2} - \sin^2 \frac{B(\chi)}{2} \right]^{1/2},$$

$$B(\chi) = 2 \arcsin \left[\sin^2 \frac{\chi}{2} - \frac{H_I^2}{4} \right]^{1/2}, \quad n=0, 1, 2, \dots$$

The functions $J_N(\chi)$, computed from the formulas (10), are shown in Fig. 2 for several values of H_I . The points of intersection of the curves $J_N(\chi)$ with the horizontal straight lines $J_N = L$ coincide with the roots of Eq. (9), and allow us to find the $\varphi_N(0) = \chi_N$ values corresponding to possible solutions of the problem for given L and H_I . The numeration of the solutions $\varphi_N(x)$, adopted in (9) and (10), coincides with the numeration of the solutions in Figs. 1 and 2.

From Fig. 2, in particular, it can be seen that the boundary-value problem (3) is nonunique: several solutions are possible for given L and H_I . After determining the values of $\varphi(0)$ from (9) or Fig. 2, we can formulate in place of the boundary-value problem (3) the equivalent Cauchy problem for Eq. (1):

$$\varphi(x)|_{x=0} = \varphi(0), \quad \left. \frac{d\varphi}{dx} \right|_{x=0} = -H_I. \quad (11)$$

The Cauchy problem (11) uniquely determines the particular solution of Eq. (1) and, moreover, if $\varphi(0)$ is defined as indicated above (the formula (9)), then a solu-

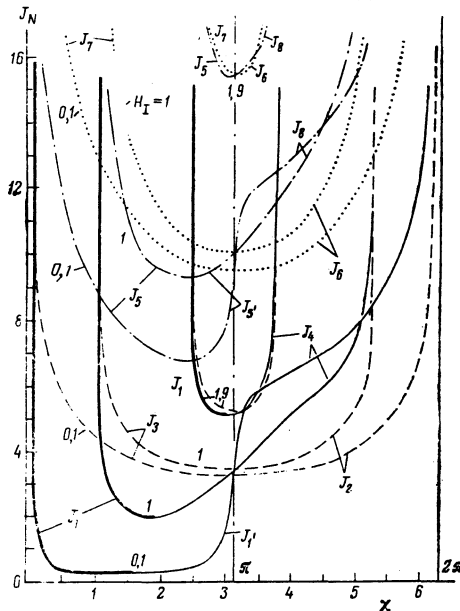


FIG. 2. The functions $J_N(\chi)$, found from the formulas (10) for different values of H_I , which are given by the numbers of the curves.

tion to the problem (11) will automatically satisfy the condition $d\varphi/dx|_{x=L} = H_I$ at the other edge of the barrier. The reduction of the boundary-value problem (3) to the Cauchy problem (11) is expedient for the computation and classification of all the possible solutions of the problem (3), as well as for carrying out numerical calculations.

3. The functions U , V , and W , determined by the formulas (10), admit of the following representations:

$$U(\chi) = 2K(z) - 2F(\psi, z), \quad V(\chi) = 4F(\psi, z), \quad W(\chi) = 4K(z), \quad (12)$$

$$z = \cos(A(\chi)/2), \quad \psi = \arcsin\{1 - H_I^2/4z^2\}^{1/2},$$

where

$$F(\psi, z) = \int_0^\psi \frac{dy}{(1 - z^2 \sin^2 y)^{1/2}}, \quad K(z) = F\left(\frac{\pi}{2}, z\right)$$

are respectively the incomplete elliptic integrals of the first kind.

In a number of limiting cases we can obtain analytic dependences in terms of elementary functions. Thus, in the vicinity of $\chi = \chi_c = 2 \arcsin(H_I/2)$ the quantity $\beta(\chi)$ in (10) becomes small. Using this fact, we find

$$U(\chi) = \ln \left[\frac{64}{\xi H_I (4 - H_I^2)^{1/2}} \operatorname{tg}^2 \left(\frac{1}{4} \chi_c \right) \right] + O(\xi). \quad (13)$$

Here $\xi = \chi - \chi_c$, and it is assumed that $\xi \ll 1$ and, furthermore, that $\xi \ll H_I(4 - H_I^2)^{1/2}$; $O(\xi)$ denotes the terms that vanish as $\xi \rightarrow 0$.

If, on the other hand, $\xi \ll H_I \ll 1$, then $\chi_c \approx H_I \ll 1$, and from (13) we obtain

$$U(\chi) = \ln(2H_I/\xi) + O(\xi). \quad (14)$$

The formulas (13) and (14) describe the behavior of the curves $J_1(\chi)$ in Fig. 2 in the vicinity of the asymptotes $\chi = \chi_c$, where the values of $J_1(\chi)$ become large.

In the case when $H_I \ll \xi \ll 1$, instead of (13), we have

$$U(\chi) = 2(2H_I/\xi)^{1/2} + O(\xi); \quad U(\chi) \rightarrow 0 \text{ as } H_I \rightarrow 0. \quad (15)$$

In the case $H_I \ll 1$, but for arbitrary values of $\xi = \chi - \chi_c$ (though when the condition $\sin \xi \ll H_I$ is fulfilled) we have

$$U(\chi) = 2H_I/\sin \xi. \quad (16)$$

This formula describes the behavior of the curves $J_1(\chi)$ in Fig. 2 for $H_I \ll 1$ and arbitrary χ , but not too close to the values $\chi = 0$ and $\chi = \pi$.

The minimum point of the $J_1(\chi)$ curves in Fig. 2 correspond at a given L to the greatest possible value, $H_{I \max}$, of the field (or to the maximum current $I_{\max} = 2H_{I \max}$). From Fig. 2 and from (16) it can be seen that for $H_I \ll 1$ the corresponding value $\chi_{\min} = \pi/2$. Substituting this value into (16), we find from the equation $L = U(\chi)$ (see (9), where $J_1 = U$) that

$$H_{I \max} = L/2, \quad L \ll 1. \quad (17)$$

Thus, for small L the maximum current through the

junction $I_{\max} = 2H_{I \max} = L$, i.e., numerically equal to the barrier width (in the dimensionless units used here).

From (9) and (16) we obtain the value of φ_0 for solutions No. 1:

$$\varphi_0 = \arcsin(2H_I/L) + H_I, \quad H_I \ll 1. \quad (18)$$

The formula (18) is valid for $L \geq 2H_I$, i.e., for $H_I < H_{\max} = L/2$.

In the case when $L \ll 1$ and $H_I \ll 1$ (though when $2H_I/L \leq 1$), instead of (18) we find with allowance for (4) that

$$\varphi_0 = \arcsin(I/I_{\max}), \quad I_{\max} = L \ll 1. \quad (19)$$

Thus, in the case of barriers of small width we obtain the normal relation between the current and the phase: $I = I_{\max} \sin \varphi_0$. In this case it is not difficult to obtain the general solution of the problem:

$$\varphi(x) = \varphi_0 - H_I x + \frac{H_I}{L} x^2, \quad H(x) = H_I \left(-1 + \frac{2x}{L} \right), \quad j(x) = \frac{2H_I}{L}, \quad (20)$$

where φ_0 is given by the formula (19).

In this case when $H_I \sim \xi = \chi - \chi_c \ll 1$ we have $\chi_c \approx H_I$ and

$$U(\chi) = \ln \frac{2H_I + \xi}{\xi}, \quad (21)$$

from which we find the value of φ_0 for the solutions No. 1:

$$\varphi_0 = H_I \frac{1 + \operatorname{ch} L}{\operatorname{sh} L} = H_I \frac{e^L + 1}{e^L - 1}, \quad H_I \ll 1. \quad (22)$$

Here it is assumed that $\varphi_0 \sim H_I \ll 1$ (i.e., the L values are not too small). In this case the general solution of the problem has the form

$$\varphi(x) = ae^x + be^{-x}, \quad H(x) = ae^x - be^{-x}, \quad j(x) = ae^x + be^{-x}, \quad (23)$$

where

$$a = \frac{H_I}{e^L - 1}, \quad b = H_I \frac{e^L}{e^L - 1}.$$

Similarly, we can derive in the limiting cases expressions corresponding to the other solutions; we shall not give them here.

In the general case of arbitrary H_I and L , Eq. (9) cannot be solved analytically, and numerical methods must be used. Figure 3 shows the numerically determined dependences of $\varphi(0)$ on H_I for $L = 1, 4$, and 9. It can be seen that the slopes of the $N = 1$ curves (solution No. 1) for low H_I satisfy the law $d\varphi_0/dH_I = (e^L + 1)/(e^L - 1)$, which follows from (22). As H_I is increased, the linear dependence (22) goes over into the steeper dependence (18), a transition process which can be followed, in particular, on the $N = 1$ curve corresponding to $L = 1$ (Fig. 3a).

4. As is clear from the foregoing, for given L and H_I there exists some set of solutions to the static boundary-value problem (1)–(3) (for example, there are

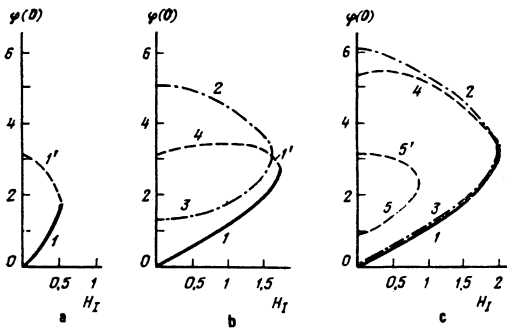


FIG. 3. H_I dependences of $\varphi(0)$ found from (9) (see also Fig. 2): a) $L=1$; b) $L=4$; c) $L=9$. The curves are labeled by the numbers, N , of the corresponding solutions (cf. the J_N curves in Fig. 2). The heavy curves correspond to stable solutions.

two solutions for $0 < L < \pi$, four for $\pi < 2\pi$, six for $2\pi < L < 3\pi$, etc. (see Figs. 2 and 3). In order that a given specific solution can be realized in the barrier, it should be stable against small perturbations. The stability of the static solutions is investigated in the following manner (cf. Ref. 5).

Instead of Eq. (1), let us consider the more general partial differential equation^[2, 5, 7]

$$\frac{\partial^2 \varphi}{\partial t^2} + \beta \frac{\partial \varphi}{\partial t} - \frac{\partial^2 \varphi}{\partial x^2} + \sin \varphi = 0, \quad (24)$$

which goes over into Eq. (1) when the time derivatives are neglected. Here t is a dimensionless time, while β is a phenomenological parameter that takes into account the dissipative losses in the barrier that are connected with the appearance of a nonstationary electric field, $E \sim \partial \varphi / \partial t$, and a normal component of the current, $j_n = \sigma E$ (σ is the normal conductivity). Let us write the time-dependent solution to Eq. (24) in the form

$$\varphi(x, t) = \varphi_0(x) + \Psi(x, t), \quad \Psi(x, t) = \psi(x) e^{i\omega t}, \quad |\Psi(x, t)| \ll 1, \quad (25)$$

where $\varphi_0(x)$ is any of the static solutions to the problem (1), (3), while $\Psi(x, t)$ is a small deviation from the static solution. Substituting (25) into (24), we find a linearized equation for the amplitude $\Psi(x)$:

$$\begin{aligned} d^2 \psi / dx^2 + v(x) \psi &= E \psi, \\ v(x) &= -\cos \varphi_0(x), \quad E = \omega^2 + \beta \omega. \end{aligned} \quad (26)$$

Since the boundary conditions (3) are assumed to be given and time independent, the solution to Eq. (26) satisfies the conditions

$$\frac{d\psi}{dx} \Big|_{x=0} = \frac{d\psi}{dx} \Big|_{x=L} = 0. \quad (27)$$

From Eq. (26) with the conditions (27) we can find the spectrum of the eigenvalues, E , of the problem. Knowing the eigenvalue E , we can find the increments determining the temporal evolution of the solutions:

$$\omega_{\pm} = -\frac{1}{2}\beta \pm (\frac{1}{4}\beta^2 + E)^{1/2}. \quad (28)$$

From (28) it is clear that for $E > 0$ there is sure to be a

growing solution of the form $\Psi \exp(\omega_{+} t)$, $\omega_{+} > 0$, i.e., such a solution is unstable. For $E < 0$ there is no growing solution, and the solution in question is stable. Thus, the problem of determining whether the static solution $\varphi_0(x)$ is stable or not reduces to the problem of finding the smallest positive eigenvalue of Eq. (26).

The numerical solution of the problem (26)-(28) showed that only the solutions No. 1, depicted in Figs. 2 and 3 by the heavy lines, are stable. All the remaining solutions turned out to be unstable (including the solutions corresponding to vortices with an oppositely directed magnetic field—solutions Nos. 5 and 6 in Fig. 1b). The conclusions drawn about the stability on the basis of the linearized equation (26) were verified by a direct numerical solution of the partial differential equation (24), and were confirmed by an investigation of the temporal evolution of the solutions. In particular, it was found that all the unstable solutions eventually become transformed under the influence of weak perturbations into stable solutions of the No. 1 type. Notice that a similar conclusion concerning the instability of the anomalous solutions is arrived at Refs. 5 and 8, where other boundary-value problems are considered. Examples of the temporal evolution of the solutions for different formulations of the problem can be found in Refs. 5, 8, and 9. Thus, in the absence of an external magnetic field in a barrier with a transport current, there cannot be vortex states (i.e., regions with oppositely directed currents). This conclusion, by the way, has been drawn only for the case of an ideal homogeneous barrier. It is possible that the inhomogeneities present in real barriers can exert a stabilizing influence on the unstable distributions, making them metastable (an effect similar to the effect whereby vortices are pinned in a type-II superconductor). We did not, however, investigate this question in greater detail.

5. As can be seen, in particular, from Figs. 2 and 3, for given L there exists some critical field value H_{Ic} (or a critical value of the total current, $I_c = 2H_{Ic}$, the problem (1), (3) possessing no static solution when $H_I > H_{Ic}$ (or when $I > I_c$). The dependence $H_{Ic}(L)$ for the No. 1 stable solutions is depicted in Fig. 4 by the continuous line. (This dependence is equivalent to the dependence $I_{\max}(L)$, whose plot is shown in Owen and Scalapino's paper^[11].) As is clear from Fig. 4, for $L \ll 1$ we have, in accord with the formula (17), the linear dependence $H_{Ic}(L) = L/2$. The dashed curve in Fig. 4 gives the critical fields for solutions Nos. 2, 3, and 5.

It is natural to ask the question: Which nonstationary solution will be established in the junction if a current strength $I > I_c$ is maintained? The answer to this ques-

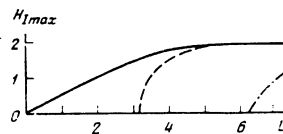


FIG. 4. Dependence of the critical field $H_{I \max}$ on L for the No. 1 stable solutions (the continuous curve; cf. Ref. 1), as well as for the unstable solutions Nos. 2 and 3 (dashed curve) and No. 5 (dot-dash curve).

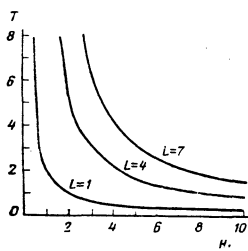


FIG. 5. Dependence on H_I of the period of the stationary self-oscillations in the barrier for $L=1, 4$, and 7 . The period of the oscillations becomes infinite at $H_I < H_{I_{\max}}(L)$ (see Fig. 4). For $H_I < H_{I_{\max}}$ a static solution is realized in the junction.

tion can be obtained with the aid of the time-dependent equation (24). The numerical calculation showed that after some time the solution got into a stable self-oscillating regime that did not depend on the initial conditions (cf. Refs. 8 and 10). The period of the stationary self-oscillations as a function of H_I is shown in Fig. 5 for $L=1, 4$, and 7 and $\beta=1$.

In Fig. 6 we show the distributions of the electric field $E = \partial\varphi/\partial t$, the superconducting current $j_s = \sin\varphi(x)$, and the magnetic field $H = \partial\varphi/\partial x$ in a junction with $L=4$ ($H_I=7$) at different moments of time encompassing the total period of the stationary self-oscillations. (In the case of Fig. 6, the period $T \approx 1.2$ and the curves follow each other downward at intervals of $\Delta t = 0.2$.) It can be seen that in the nonstationary regime there are realized in the junction current distributions that are similar to the anomalous unstable solutions of the static problem (compare the curves for the current in Fig. 6 with the curves for the solutions 4 and 5 in Fig. 1c).

Notice that in the above-considered formulation of the problem the magnetic field at the junction edges is assumed to be time-independent ($H = \pm H_I = \text{const}$). This means that outside the barrier the magnetic field parallel to the surface of the conductor is also constant. In view of this, there arises the question whether under such conditions the barrier can emit electromagnetic waves even if it is in the nonstationary regime (when $I > I_c$). We shall present qualitative arguments showing that the emission is nevertheless in principle possible. Indeed, integrating Eq. (24) over the coordinate x , we obtain

$$I(t) + I_d(t) = 2H_I, \quad (29)$$

where

$$I(t) = \int_0^L (j_s + j_n) dx, \quad I_d(t) = \int_0^L \frac{\partial^2 \varphi}{\partial t^2} dx, \\ j_s = \sin \varphi, \quad j_n = \beta \partial \varphi / \partial t.$$

As can be seen from (29), the constancy of the magnetic field $\pm H_I$ at the junction boundaries is guaranteed by the presence in the junction, besides the electric current $I(t)$, of a displacement current, $I_d(t)$, which appears when $\partial F/\partial t \sim \partial^2 \varphi/\partial t^2$ has a nonzero value in the barrier. Thus, the electric current, $I(t)$, connected with charge transport in the system is time-dependent. Therefore, charge oscillations occur in a circuit con-

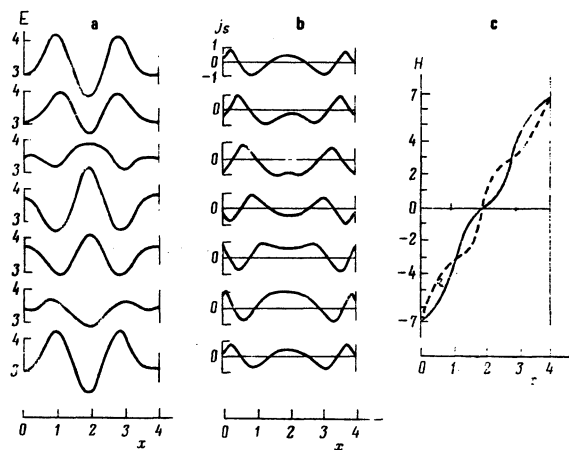


FIG. 6. An example of a self-oscillatory process in a Josephson junction with $L=4$, $H_I=7$, and $\beta=1$. a) Distribution of the electric field $E = \partial\varphi/\partial t$, and b) distribution of the current $j_s = \sin\varphi$, at different moments of time. The E and j_s distributions shown follow each other (downward) at time intervals $\Delta t = 0.2$, and cover the full period, $T \approx 1.2$, of the self-oscillations. c) Two limiting $H = \partial\varphi/\partial x$ field distributions (the continuous and dashed curves), shifted in time by a half-period $\frac{1}{2}T \approx 0.6$. The self-oscillations of the H field occur in the region enclosed by the indicated curves.

taining a Josephson junction operating in a nonstationary regime, and such a system can, in principle, radiate. However, in the above-considered regime ($H_I = \text{const}$) only the magnetic-field component perpendicular to the current can vary. This condition imposes its own limitations, in particular, on the polarization of the radiation coming out of the barrier. The detailed consideration of the radiation of such a system requires the use of a more complete system of equations, and falls outside the limits of the present paper.

Let us note in conclusion that the above-indicated distinctive features of the dynamic solutions can be used to analyze the operations of SKVID's in the nonstationary regime.

- 1) We shall call such type of current states "normal." In Ref. 1 only such normal states are investigated (see also Solymar's book,^[2] where Owen and Scalapino's results are used for a qualitative description of the phenomena connected with the stationary Josephson effect).
- 2) Solutions of Eq. (1) that increase with the coordinate are realized in a barrier located in an external field, and do not arise in the present problem (cf. Refs. 4 and 5).

¹C. S. Owen and D. J. Scalapino, Phys. Rev. **164**, 538 (1967).

²L. Solymar, Superconducting Tunneling and Applications, John Wiley, New York, 1972 (Russ. Transl., Mir, 1974).

³I. O. Kulik, Zh. Eksp. Teor. Fiz. **51**, 1952 (1966) [Sov. Phys. JETP **24**, 1307 (1967)].

⁴G. F. Zharkov, Zh. Eksp. Teor. Fiz. **71**, 1951 (1976) [Sov. Phys. JETP **44**, 1023 (1976)].

⁵G. F. Zharkov and S. A. Vasenko, Zh. Eksp. Teor. Fiz. **74**, 665 (1978).

⁶R. A. Ferrell and R. E. Prange, Phys. Rev. Lett. **10**, 479 (1963).

⁷I. O. Kulik and I. K. Yanson, Éffekt Dzhozefsona v sverkhprovodyashchikh tunnel'nykh strukturakh (The Josephson Effect in Superconducting Tunneling Structures), Nauka,

Fluctuations of the surface potential in metal-insulator-conductor structures

V. A. Gergel' and R. A. Suris

(Submitted 21 December 1977)

Zh. Eksp. Teor. Fiz. **75**, 191-203 (July 1978)

The potential relief of the semiconductor-insulator interface, due to the inhomogeneity of the charge in the insulator, is investigated in MIS structures. Assuming no correlation between the positions of the charged centers and taking into account charge-density fluctuations of all scales, the mean squared fluctuations of the surface potential are determined as functions of the character of the location of the built-in charge in the interior of the insulator and of the electron density. The effective density of the surface electronic states due to the potential fluctuations is obtained, as well as the temperature dependence of the surface conductivity of the MIS structure.

PACS numbers: 73.40.Qv, 73.20.-r, 73.25.+i

In the overwhelming majority of cases, the threshold voltages of the characteristics of MIS (metal-insulator-semiconductor) structures and of devices on their basis are shifted as a result of the presence of a certain fixed charge in the insulator layer. This "built-in" charge causes a corresponding bending of the bands in the surface region of the semiconductor in the absence of an external bias. Its magnitude is characterized by the so-called flat-band voltage, i.e., the voltage that must be applied to the metallic electrode of the structure to compensate for the action of the built-in charge on the semiconductor. It is clear beforehand that the density of the built-in charge is not uniform over the area of the MIS structure. One of the causes of the inhomogeneity is the imperfection of the methods used to prepare the MIS structure. However, even at the most perfect technology, there remain statistical fluctuations due to the discrete character of the elementary charge. The inhomogeneity of the built-in charge, causing corresponding fluctuations of the surface potential of the semiconductor, can lead generally speaking to much more substantial changes of the capacitive and current characteristics of the MIS structures than a simple additive shift along the voltage axis. In fact, consider by way of example an MIS structure at $T = 0$, in which the average surface potential corresponds to depletion of the majority carriers from the surface layer (see Fig. 1). The Fermi level on the surface lies in this case much lower than the average position of the bottom of the conduction band. In the homogeneous case the surface concentration of the carriers at such a bending of the bands would be zero. However, because of the inhomogeneity of the built-in charge, the position of the edge of the band fluctuates, and the bands cross the Fermi level in individual sections of the surface. In these sections, a certain electronic charge is accumulated, so that the

average electron density becomes finite. It is clear that with increasing bending of the bands the fluctuation amplitude needed for the formation of the electron "drop" decreases, the probability of such a crossing increases, and the average electron density increases. The actual situation is somewhat more complicated, since the amplitude of the fluctuations is, on account of screening, itself dependent on the electron density, whose value must be determined in self-consistent fashion. The electrons, which accumulate in the minima of the potential relief, partially screen the semiconductor volume, and this decreases the total-voltage fraction across the space-charge layer, and leads therefore to an increase of the capacitance of the MIS structure, similar to what occurs when the surface states are filled.^[1] Thus, one of the experimental manifestations of the fluctuations of the built-in charge may be deformation of the $C-V$ characteristics of the MIS structure.

Another manifestation of the fluctuations of the built-in charge is a characteristic dependence of the surface conductivity on the temperature and on the bias voltage. In fact, when fluctuations are present the surface electrons are located mainly at minima of the surface relief. Therefore the flow of current in the system requires the surmounting of potential barriers, and

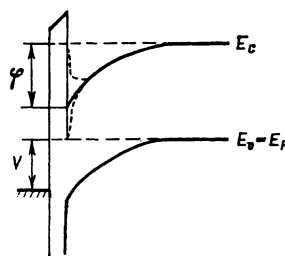


FIG. 1.